Experimental Transplantation of Carcinoma to Tooth Extraction Sockets: A bone invasion model

Hideki Takahashi, Tsugio Inokuchi, Hisazumi Ikeda, Joji Sekine and Akihiko Irie

Division of Oral and Maxillofacial Surgical Reconstruction and Functional Restoration,Department of Developmental and Reconstructive Medicine, Graduate School of Biomedical Sciences, Nagasaki University, Nagasaki, Japan

Takahashi H, Inokuchi T, Ikeda H, Sekine J and Irie A. Experimental transplantation of carcinoma to tooth extraction sockets: A bone invasion model. *Oral Med Pathol* 2003; 8: 61-69, ISSN 1342-0984

The purpose of this study was to delineate the process of bone invasion by oral carcinoma. An experimental model of oral carcinoma invading jawbone was established by transplanting mouse NR-S1 tumor or human-cultured NB-1 tumor to the tooth extraction socket. In the early stage after tumor transplantation, the tumor grew in the extraction socket and subsequently filled the socket and extended outward to the neighboring regions. Bone resorption and collagen production status, as well as HSP47 expression, were investigated in the process of the tumor invasion. Osteoclasts appeared increasingly on the surface of the corresponding bone during the early stage and then decreased in number as bone resorption with tumor invasion progressed. Enlarged osseous lacunae, as well as Haversian and Volkmann's canals, were present in the bone near the tumor, and tumor cells were also detected in the enlarged osseous spaces. Expression of HSP47 was positive for the carcinoma cells infiltrating into the bone tissue, but not for the counterparts in the mass. In summary, cells may invade bone through the osteolytic spaces and necessitate ECM around them for their nutritional supply to proliferate.

***Key words*: animal model of oral carcinoma, bone resorption, osteoclast, HSP47**

***Correspondence*: Hideki Takahashi,** Division of Oral and Maxillofacial Surgical Reconstruction and Functional Restoration, Department of Developmental and Reconstructive Medicine, Graduate School of Biomedical Sciences, Nagasaki University1-7-1 Sakamoto, Nagasaki 852-8588, Japan

Phone: +81-95-849-7704, Fax: +81-95-849-7705, E-mail: hideki807@giga.ocn.ne.jp

Introduction

Gingival carcinoma often causes destruction of the jawbone (1-4). An understanding of the patterns and routes of carcinoma invasion into jaw- bone is essential in determining and deciding the appropriate surgical margin of jaw resection.

Generally, bone resorption is considered to be mediated by osteoclasts. Recently the possibility of osteolysis by factors derived from the osteocytes or the tumor itself has also been suggested (5, 6). In addition, many recent reports have described enlargement of lacunae with proliferation of the tumor in the area of the bone adjacent to the tumor (7). It has also been suggested that this enlargement of osseous lacunae is closely related to the death of osteocytes (5, 8, 9) and is caused by osteolysis due to the death of osteocytes (8, 9). However, whether bone is resorbed not only by osteoclasts but also by other factors remains controversial (10-14).

Previous study has indicated that as the tumor invades the bone, a layer of collagen is formed between the tumor and the surface of the bone, and that collagen fibers are also presented in resorption pits and around tumor cells which have invaded the bone (7). The interaction of tumor cells with the ECM (extracellular matrix) plays a central role in the multistep process of tumor invasion (15). Recent studies have shown that the tumor cells synthesize collagen, which is the main component of the ECM (16, 17).

The purpose of this study was to use a mouse model of oral carcinoma in order to observe the process of bone invasion, and to determine whether collagen synthesis is the nutritional mediator for the tumor invading the bone.

Material and Methods

Animals and materials

All animal experiments were carried out in accor-

dance with the guidelines for animal experimentation of the Laboratory Animal Center for Biomedical Reseach, Nagasaki University School of Medicine.

I. NR-S1 model

Animals: Five-week-old male C3H/He mice (body weight 17-20g, n = 30, Charles River, Japan) were used. To minimize tissue injury due to tooth extraction, the mice were fed powdered food containing ß-aminopropionitrile (ß-APN, Sigma Chemical Co. U.S.A.) at a concentration of 0.4% for 5 days (18). The mice were then anesthetized with sodium pentobarbital (0.05mg/g), and the left maxillary incisor was extracted with the use of an exploratory needle and a mosquito forceps. Gauze and pressure were applied to the wound to promote hemostasis.

Tumors: Transplantable NR-S1 tumor, which was derived from the buccal mucosa of a C3H mouse (19, 20)(National Institute of Radiological Sciences, Chiba, Japan) was used. The pathological features showed well-differentiated squamous cell carcinoma. The NR-S1 tumor was serially passaged in the subcutaneous region of the mouse femur.

Tumor transplantation into the extraction socket

Twenty days after tumor transplantation, the subcutaneously proliferated NR-S1 tumor mass was harvested, washed with sterilized physiological saline solution, and minced into a piece measuring about $1mm^3$. One piece of this tumor was transplanted into the extraction socket of the left maxillary incisor of each animal.

II. NB-1 model

Animals: Four-week-old BALB/cANcrj female nude (nu/nu) mice(body weight 17-20g, n = 7, Charles River, Japan) were used.The mice were housed three per cage and kept under specific-pathogen-free conditions, and they were used for the experiments when they were five weeks old.

Tumors: Cultured tumor cell line NB-1 was established in the Second Department of Oral and Maxillofacial Surgery, Nagasaki University, from a 70-year-old Japanese male patient with squamous cell carcinoma of the left buccal mucosa (unpublished).

To establish a transplantable tumor from this *in vitro* cell line, tumor cells were subcutaneously injected into the femoral region of nude mice using a 27G needle (20 mice, 1×10^7 cells per mouse). Thirty days after tumor transplantation, the subcutaneously proliferated NB-1 tumor mass was harvested and transplanted into the extraction sockets of nude mice, same as for the NR-S1 tumor.

Tissue preparation

I. NR-S1 model

The mice were euthanized with an overdose of pentobarbital sodium at 1, 2, 3, 5, 7, 9, 11, 13, and 15 days after tumor transplantation.

A group of three mice receiving no tumor transplant served as the control. The head and neck were harvested and fixed in 10% neutral buffered formalin for 24 hours. Subsequently, the maxilla, including the extraction socket, was cut with a diamond band saw (EXACT, Germany) into frontal sections (n = 3, each) measuring 3 to 5 mm in thickness. The sections were decalcified with 10% EDTA-2Na solution (WAKO, Japan) at 4°C for 10 days. The specimens were embedded in paraffin and sliced into continuous 4-µm-thick sections according to routine procedures.

II. NB-1 model

The results of the preliminary experiments indicated that NB-1 tumor transplanted into the extraction sockets grew more slowly compared with NR-S1 tumor. The mice were euthanized at 30 days after tumor transplantation. Others procedures were performed as described for the NR-S1model.

TRAP staining

TRAP staining was performed as described by Barka *et al.* (21). A mixture of N, N-dimethylformamide (WAKO, Japan) and 1.2 mM naphthol AS-MX phosphate (Sigma Co., St. Louis, MO, USA) was used as the substrate. To prepare the reaction solution, pararosanilin (WAKO, Japan) and concentrated hydrochloric acid were added to 0.1 M sodium acetate buffer (pH 5.0) solution. Sodium nitrite solution 4% was added, the mixture was allowed to stand at room temperature for 1 to 2 minutes, and it was then added to the substrate. The pH was adjusted to 5.0 with 1 NNaOH, and L-dihydrosuccinic acid was added. The mixture was allowed to react at 37°C for 90 min. The number of TRAP-positive cells per 1 mm of bone surface adjacent to the tumor was counted under a light microscope at a magnification of 400 times with the use of a squared eyepiece graticule (Nikon, Tokyo, Japan).

Immunohistochemical staining

***In Vivo* experiment**: Paraffin sections were dewaxed in xylene and rehydrated in a graded ethanol series. The slides were incubated with 0.3% hydrogen peroxide in methanol for 30min to quench endogenous peroxidase activity and treated with 0.1% trypsin solution (Sigma Co., St. Louis, MO, USA) in 0.05M Tris buffer, pH7.6 at room temperature for 10 min.

After five washes in cold phosphate buffered saline (PBS, pH7.2) for 10 minutes each, non-specific binding was blocked by 1.5% skimmed milk in PBS including normal blocking serum. The sections were allowed to react with the primary antibodies and were incubated for 24h at 4°C.

The antibodies and dilutions used are shown in Table 1. As a negative control, the primary antibodies

Table 1: Primary antibodies used in this study

Antibody	Type	Dilution(NR-S1/NB-1)	Source
HSP47	monoclonal	1:1000/ 1:2000	Biotechnologies Corp, Canada
Collagen Type I	polyclonal	1:100/1:250	LSL Co. LTD, Japan
Collagen Type III	polyclonal	1:200/1:800	Santa Cruz Biotechnology, USA
VEGF	polyclonal	1:350/1:200	Santa Cruz Biotechnology, USA

were replaced by PBS. After washing with PBS, the sections were incubated for 30min each in diluted biotinated secondary antibody and avidin-biotin complex reagent (Vectastain, Vector, Burlingame, CA, USA). They were then washed again in PBS and finally the slides were incubated in a substrate solution consisting of 0.05% diaminobenzidine tetrahydrochloride (DAB) and 0.05% hydrogen peroxide in 0.05M Tris-buffer solution (pH 7.6). Counterstaining was done with Mayer's hematoxylin for 30 seconds. A portion of the continuous sections was stained with 1% methylgreen and hematoxylin and eosin.

***In Vitro* experiment**: NB-1 cells were cultured on the chamber slides. The cells were fixed by absolute ethanol and processed for immunohistochemical staining the same as in the *in vivo* experiment.

Western blotting

Expression of HSP47 (Heat shock protein 47) in NB-1 tumor cells were determined by Western blotting. Culture cells were solubilized in lysis buffer. Protein samples (10μg) were applied to 10% SDS-PAGE and blotted onto nitrocellulose membrane (Bio Trace NT Blotting Membrane, Gelman Science, Japan). After blocking nonspecific binding with 3% skimmed milk in TBS-T (pH7.4, containing 1% Tween20) for 30min at room temperature, the blotted membranes were incubated with mouse anti-HSP47 antibody (StressGen Biotechnologies Corp, Canada. 30000:1) overnight at 4°C, followed by incubation with peroxidase conjugated anti-mouse IgG for 1 hour at room temperature. The membranes were treated with ECL Western blotting detection reagents (Amersham, Arlington Heights, IL, USA) and exposed to ECL film.

TUNEL staining

Apoptotic cells were examined *in situ* by means of the terminal deoxynucleotidyl transferase (TdT)-mediated dUTP-biotin nick-end labeling (TUNEL) method (22), with the Oncor Apoptosis Detection Kit peroxidase (Apoptag-Plus Oncor, Gaithersburg, MD, USA) according to the manufacturer's protocol. On sections used as negative controls for the specificity of labeling, distilled water was substituted for the TdT enzyme.

Results

I. NR-S1 model

Day 1 after tumor transplantation

The tooth extraction socket was filled with blood coagula. The transplanted tumor piece was observed to be surrounded by blood coagula with inflammatory cell infiltration in the extraction socket. The tumor cells varied in size and were polygonal in feature, and their nuclei were elliptical, relatively large, and densely stained by hematoxylin. Some cells were revealed to be mitotic. Degenerative or necrotic cells were also demonstrated. The extraction socket showed well-defined boundaries with a smooth inner surface of the bone.

Day 2 after tumor transplantation

The tumor tissue grew in the extraction socket and showed marked alveolar formation. Many tumor cells showed mitosis. Around the margin of tumor tissue, infiltration of inflammatory cells, such as lymphocytes and mast cells, were more notable than after transplantation day 1. The presence of osteoblasts on the surface of alveolar bone was demonstrated away from the location of the tumor.

Day 3 after tumor transplantation

The tumor tissue massively proliferated further, filling the extraction socket and showing central necrosis (Fig. 1). Also, tumor cells infiltrated into periodontal ligament remnants and, further, into alveolar bone.The surface of bone in areas adjacent to the tumor tissue showed sporadic resorption pits containing osteoclasts (Fig. 2). The Haversian canals and osseous lacunae of alveolar bone showed mild enlargement in areas adjacent to the tumor tissue.

Days 5 to 7 after tumor transplantation

Tumor tissue filling the extraction socket extended to the neighboring regions. The tumor tissue and the al-

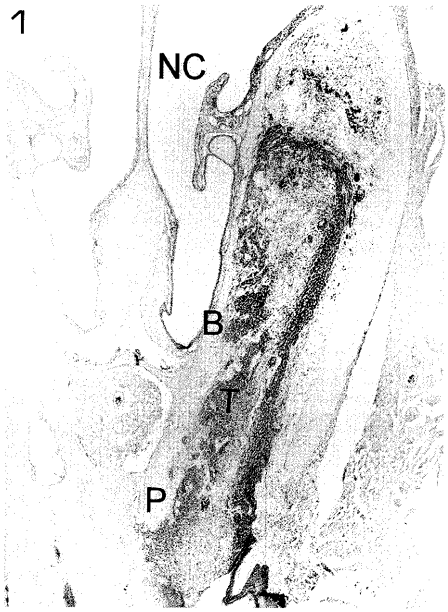

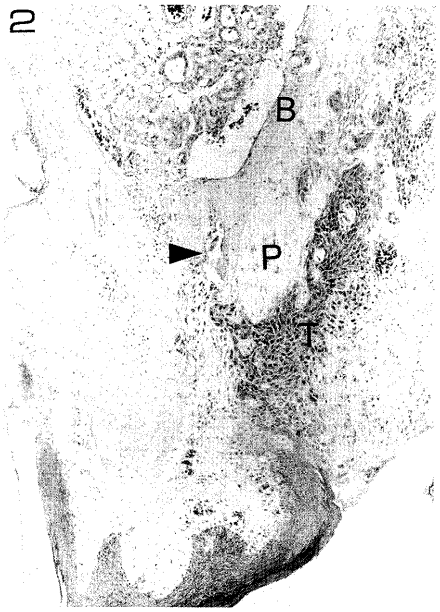

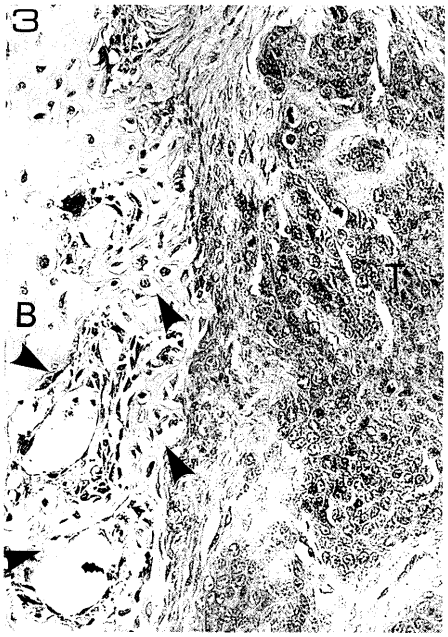

Fig. 1: Tumor tissue can be seen adjacent to the periodontal ligament remnant and bone surface. At the bottom of the extraction socket, inflammatory cells are present. Day 3 after NR-S1 tumor transplantation. (HE stain, ×10) (P: periodontal ligament remnant, B: alveolar bone, T: tumor cells, NC: nasal cavity)

Fig. 2: High-power view of Fig. 1. The tumor is invading into the periodontal ligament and bone (arrow head). Day 3 after NR-S1 tumor transplantation. (HE stain, ×25) (P: periodontal ligament remnant, B: alveolar bone, T: tumor cells)

Fig. 3: A large number of enlarged osseous lacunae. Enlargement of osseous lacunae and Haversian and Volkmann's canals was observed, combined with resultant large resorption spaces (arrow head).Day 7 after NR-S1 tumor transplantation. (HE stain, ×80) (B: alveolar bone, T: tumor cells)

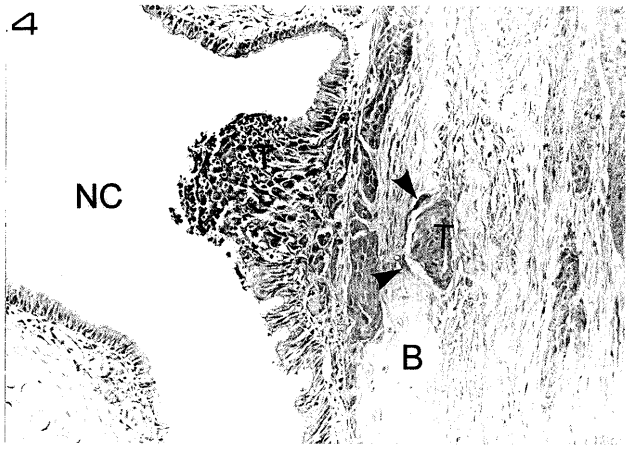

Fig. 4: Tumor extending to the nasal cavity with bone destruction. Osteoclasts are present on the medial surface of the bone (arrow head). Day 9 after NR-S1 tumor transplantation. (HE stain, ×50) (B: alveolar bone, T: tumor cells, NC: nasal cavity)

veolar bone were separated by relatively thick fibrous connective tissues, where marked lymphocyte-dominant inflammatory cell infiltration was observed.

Fibrous tissues were observed around the tumor, which varied from massive tissue to single cells. Also, proliferation of blood vessels was observed in the connective tissues around the tumor. In the alveolar bone adjacent to the tumor tissue, resorption pits with osteoclasts on the surface of bone and vermicular bone resorption became more notable and extended further than before. Enlargement of osseous lacunae and Haversian and Volkmann's canals were present, combined with resultant large resorption spaces (Fig. 3).

Days 9 to 11 after tumor transplantation

The tumor extended towards the nasal cavity (Fig. 4), proliferating as cords or lumps and destroying the remaining alveolar bone (Fig. 5-A). Tumor cells infiltrating into the enlarged osseoue spaces were demonstrated.

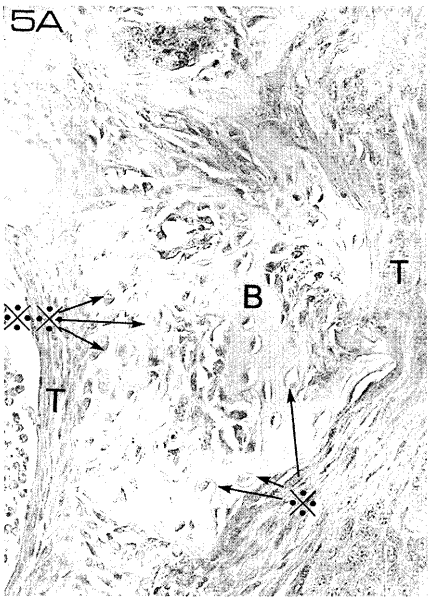

Fig. 5A: Alveolar bone surrounded by tumor. Enlarged lacunae are seen in the bone. Some tumor cells are locating in the enlarged lacunae. Day 13 after NR-S1 tumor transplantation. (HE stain, ×80)(B: alveolar bone, T: tumor cells, ※: enlarged lacunae, ※※: tumor cells locating in the enlarged lacunae)

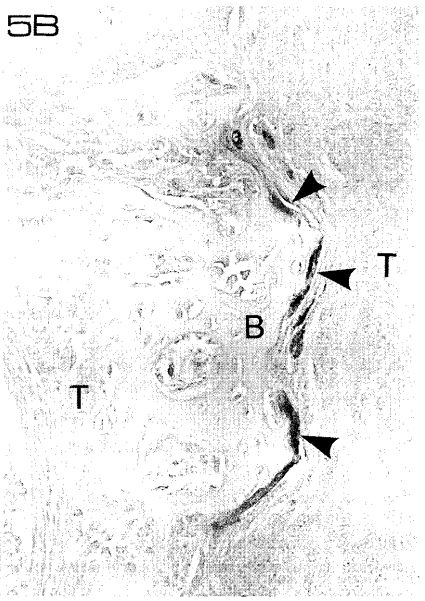

Fig. 5B: TRAP-positive osteoclasts (arrow head) on the surface of the bone.Day 13 after NR-S1 tumor transplantation. (TRAP stain, ×80) (B: alveolar bone, T: tumor cells)

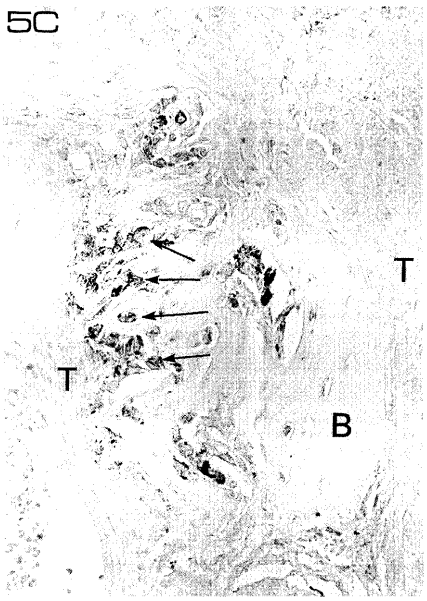

Fig. 5C: HSP47-positive tumor cells within the bone (arrow). Day 13 after NR-S1 tumor transplantation. (HSP47 stain, ×80)(B: alveolar bone, T: tumor cells)

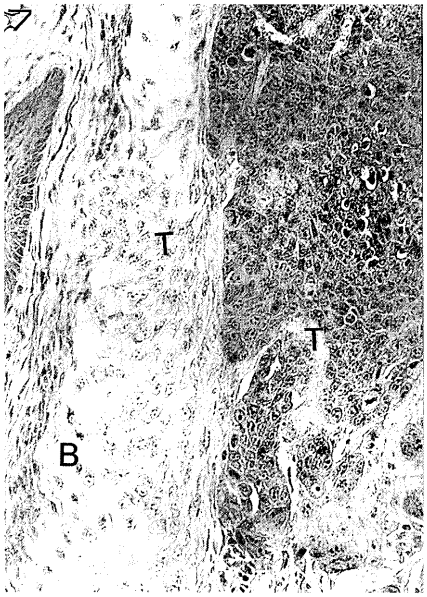

Fig. 7: Tumor tissue invading bone in a vermicular pattern at its invasive front. Osteoclasts were not observed. Day 11 after NR-S1 tumor transplantation. (HE stain, ×80) (B: alveolar bone, T: tumor cells)

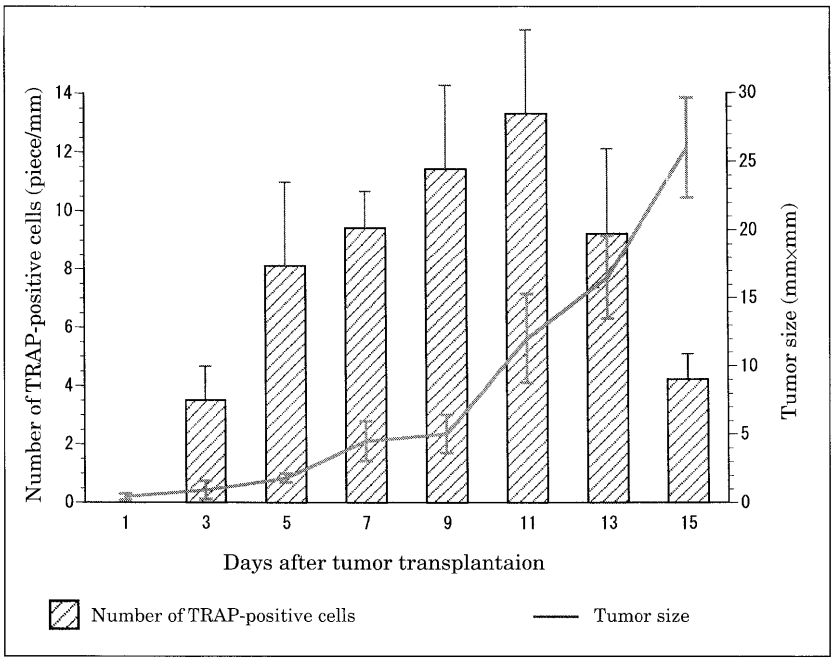

Fig. 8: The number of TRAP-positive cells per 1 mm of bone surface adjacent to the proliferating NR-S1 tumor.

There was also evidence of tumor invasion into the musculature. TRAP-positive cells were seen in some areas along the bone surface adjacent to the tumor mass (Fig. 5-B). Contrary to the tumor cells in the mass, the tumor cells occupying the enlarged bone spaces were revealed to be HSP47-positive (Figs. 5-C, 6-A). Positive staining for HSP47 was also found in fibroblasts in the tumor interstices and in the fibroblasts around the tumor mass (Fig. 6-A). A type III collagen-positive area was observed around the tumor (Fig. 6-B). On the other hand, osteoblastic new bone formation was also observed sporadically on the outer surface of the extraction socket.

Days 13 to 15 after tumor transplantation

The alveolar bone was almost destroyed by the tu-

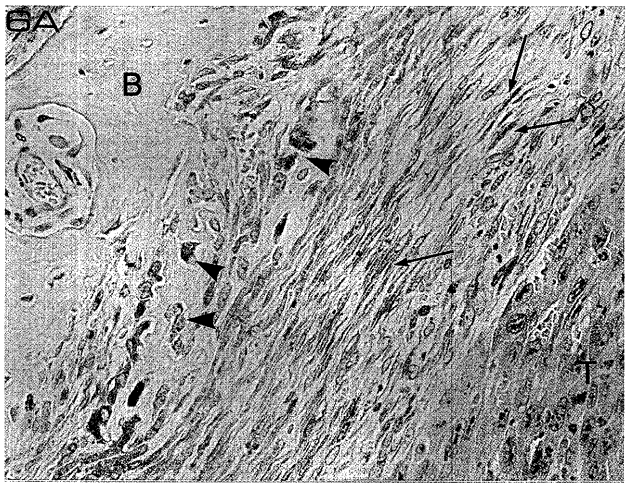

Fig. 6A: Tumor cells (arrow head) infiltrating into the bone and fibroblasts (arrow) adjacent to the tumor mass are HSP47- positive. Day 11 after NR-S1 tumor transplantation. (HSP47 stain, ×100) (B: alveolar bone, T: tumor cells)

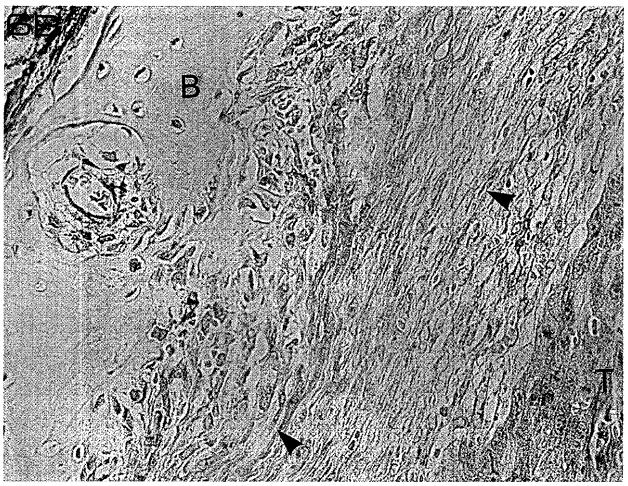

Fig. 6B: Collagen type -III positive images are seen around thetumor (arrow head). Day 11 after NR-S1 tumor transplantation. (Collagen type III stain, ×100) (B: alveolar bone, T: tumor cells)

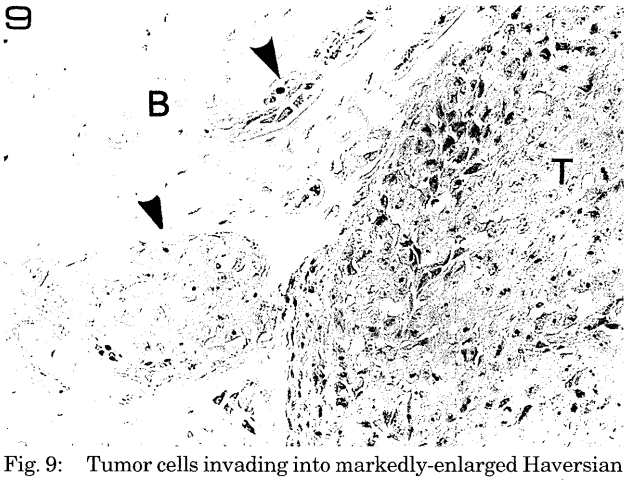

Fig. 9: Tumor cells invading into markedly-enlarged Haversian and Volkmann's canals and microalveoli (arrow head). Day 30 after NB-1 tumor transplantation. (HE stain, ×80) (B: alveolar bone, T: tumor cells)

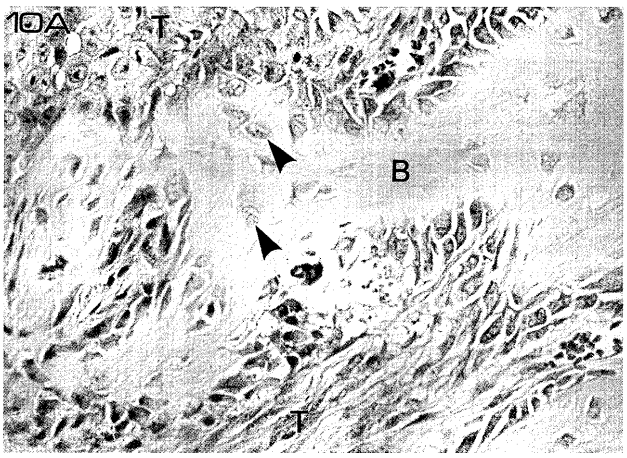

Fig. 10A: Tumors cells locating in the enlarged lacunae (arrow head). Day 30 after NB-1 tumor transplantation. (HE stain, ×160) (B: alveolar bone, T: tumor cells)

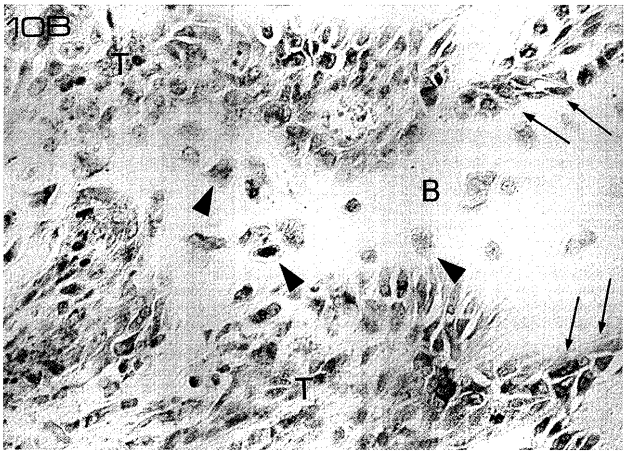

Fig. 10B: HSP47-positive tumor cells (arrow head). HSP47-positive osteoblasts (arrow). Day 30 after NB-1 tumor transplantation. (HSP47 stain, ×160) (B: alveolar bone, T: tumor cells)

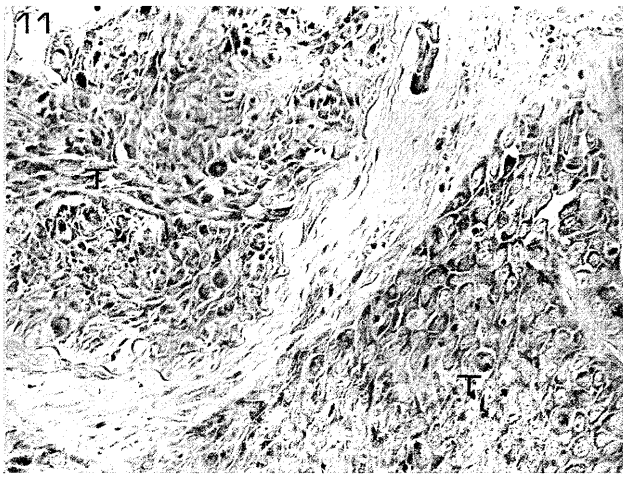

Fig. 11: VEGF-positive NR-S1 tumor cells.2 Day 9 after NR-S1 tumor transplantation. (VEGF stain, ×80) (T: tumor v cells)

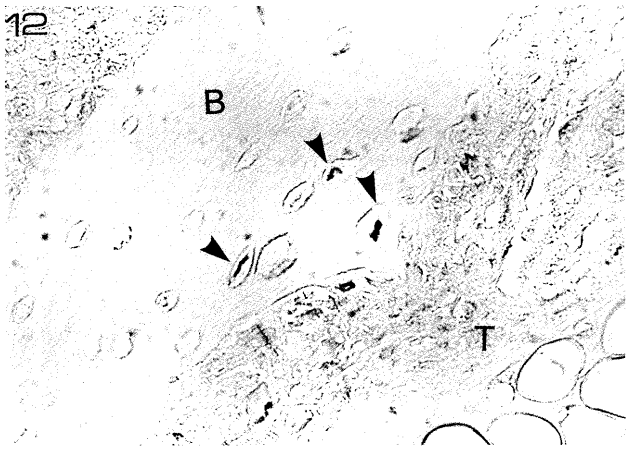

Fig. 12: TUNEL-positive osteocytes in the area approach by the tumor (arrow head), and empty osseous lacunae. Day 7 after NR-S1 tumor transplantation. (TUNEL stain, ×160) (B: alveolar bone, T: tumor cells)

mor. Vermicular pattern of bone invasion at the tumor front was demonstrated, where no osteoclast was present (Fig. 7). Nearly almost all of the tumor cells occupying the osteolytic bone spaces were HSP47-positive.

TRAP-positive cells

The number of TRAP-positive cells (osteoclasts) counted in the time course is shown in Figure 8. The number of osteoclasts increased together with the tumor growth, reached a peak at 11 days, and then decreased.

II. NB-1 model

In Vitro study of NB-1 cells

NB-1 cells were immunohistochemically positive for HSP47, and HSP47 protein was confirmed in these cells by Western blotting analysis.

Day 30 after tumor transplantation

Seven animals showed metastasis to the cervical lymph nodes.

Tumor filled the extraction socket and proceeded to the outside of the alveolar bone and to the nasal cavity. Vigorous mitotic activity was indicated and few necrotic areas were noted. Varied quantities of fibrous connective tissues were shown between the bone resorption surface and invading tumor mass. Osteoclasts were present on the surface of the alveolar bone and formed resorption pits. Marked enlargement of osseous lacunae and Haversian and Volkmann's canals was observed in the region adjacent to the tumor.

It was evident that the tumor cells invaded these osseous spaces and formed microalveoli in some areas (Fig. 9). Also, the formation of new bone was observed, with a large number of osteoblasts on the bone surface. Tumor infiltration into this newly formed bone was also demonstrated. Positive staining for HSP47 was found in fibroblasts in the tumor interstices and in the connective tissue around the tumor mass. HSP47- positive cells were detected in almost all of the tumor cells infiltrating into the bone. (Figs. 10-A, 10-B). No HSP47-positive tumor cell was detected in the tumor mass locating away from the bone. HSP47 -positive image was also present in osteoblasts (Fig. 10-B). Type III collagen-positive findings were observed around the tumor mass, as seen in the NR-S1 model. Type I collagen-positive findings were not detected in the tumor interstices, as observed in the NR-S1 model.

VEGF expression in NR-S1 and NB-1 tumor

VEGF (Vascular endothelial growth factor) -positive cells were demonstrated both in NR-S1 and NB-1 tumors. (Fig. 11)

TUNEL-positive osteocytes

In the NR-S1 model, some TUNEL-positive osteocytes were observed in the alveolar bone both on the non-extracted and extracted site at 1 to 3 days after tumor transplantation. From 5 days after tumor transplantation, TUNEL-positive osteocytes and empty osseous lacunae were increasingly revealed in the area approached by the tumor (Fig. 12).

In the NB-1 model, TUNEL-positive osteocytes and empty osseous lacunae were demonstrated similarly to NR-S1 model at 30 days after tumor transplantation.

Discussion

Oral squamous cell carcinomas are highly-invasive lesions that destroy adjacent tissues and invade bone. Carcinogens or transplantable tumors have been used in experimental bone invasion models of oral carcinoma (7, 19, 23-25). Carcinogens such as 9,10-dimethyl 1,2-benzanthracene (DMBA) and 4-nitroquinoline N-oxide (4-NQO) are often used to experimentally induce carcinoma (7, 25). However, they all have shortcomings, such as complex preparation procedures, and such carcinogens require a long duration for establishment of an animal model, making it difficult to obtain a standardized model. Many studies on tumor invasion using a transplantable tumor, such as mouse NR-S1 tumor (19), VX2 tumor (23), and VX7 tumor (24), have been reported. To make an experimental model for gingival carcinoma invading bone tissue, a piece of tumor was transplanted directly into the extraction socket in the present study. No model of a tumor transplanted into an extraction socket has previously been reported.

Our study showed that the number of osteoclasts increased during the early stage after tumor transplantation. However the number of osteoclasts showed a tendency to decrease in accordance with the tumor progression. Enlarged osseous lacunae, as well as Haversian and Volkmann's canals, were present in the bone approached by the tumor, and were combined with resultant larger osseous spaces. Tumor cells invaded and proliferated in these spaces and infiltrated destructively into the interior of bone.With the progress of tumor growth, osteoclast was not observed in some areas where the tumor was invading the bone. These findings are consistent with

the report by Galasko *et al.* (26) in which osteoclasts aggregated on the bone approached by the tumor but subsequently disappeared once the tumor had grown sufficiently large to envelop the bone, while bone destruction continued (the two principal mechanisms) (7, 26, 27).

It is widely accepted that osteolysis associated with malignant tumors is mediated by osteoclasts, which seem to be activated by cytokines secreted directly by tumor cells or indirectly through osteoblasts (11, 28-31). Recently, it has been reported that procathepsin L, which is well known to be a lysosomal cystein proteinase and MMP (matrix metalloproteinase) secreted from OSCC (oral squamous cell carcinoma), may be activated at the front of bone invasion, degrading the bone matrix (6, 32). However, whether bone is directly resorbed by tumors remains a matter of debate (10, 26, 27). Osteocytes are communicated via gap junctions, which are thought to ensure an adequate supply of molecules and ions (33). Galasko *et al.* (26) have reported that tumor proliferation may be responsible for thrombosis of the vessels and ischemia in the bone tissues. Recently, Hamaya *et al.* (9) reported that as a result of malnutrition of osteocytes, irreversible ischemia and hypoxia occur in osteocytes, triggering the death of osteocytes. Based on these reports, it is suggestive that the apoptotic osteocytes revealed in the present study are resulted from an impaired supply of nutrition via gap junctions. Usui *et al.* (8) also noted that necrotic osteocytes were observed under conditions of ischemia, that the release of lysosomal enzymes resulting from necrosis may destroy the surrounding bone matrix, and that subsequently the lacunae are enlarged (osteolysis) (8). Regarding necrosis of osteocytes, Hirsch *et al.* (34) proposed "secondary necrosis", in which apoptotic cells undergo necrosis if they are not quickly phagocytosed. Many empty and enlarged osseous lacunae observed in our present study are likely to be resulted from this osteolytic process.

The process of tumor invasion involves adherence of tumor cells to the ECM, degradation of matrix components, and movement of the cell body (15). Thus the surrounding ECM, collagen in particular, plays an important role in the tumor invasion. Regarding ECM surrounding the tumor, some reports have described hyperplasia of collagen, especially types I and III (35). Type I collagen is located in tumor interstices and bone tissue (35). In our experiment, collagen type III-positive regions were noted around the tumor cells, while collagen type I was mostly seen in the bone tissue and skin, and was rarely seen in tumor interstices. This difference may be because the expression of collagen varies depending on the differences in the behavior of tumors (36).

The expression of HSP47 is closely-related to that of collagen, which is the main component of ECM (37, 38). Recently it has been reported that the expression of HSP47 in the tumor is an important marker for tumor malignancy and invasion potential (37-39). In our results, all the tumor cells *in vitro* showed expression of HSP47. In contrast, the tumor tissue subcutaneously implanted was expressed to be HSP47-negative (data not shown). Regarding the tumor implanted into the sockets, however, the expression of HSP47 was positive for the tumor cells infiltrating into the bone tissue, but not for the counterparts forming the tumor mass.

On the other hand, VEGF expression (40) was found in the tumor cells, both in the bone and tumor mass. Therefore, it may be conceivable that the tumor cells necessarily induce collagen production which mediates nutrition for their survival in the bone tissue, progressively composing the massive structure with interstices and vasculature.

In summary, carcinoma cells may invade the bone through the osteolytic spaces and necessitate ECM around them for nutritional supply to proliferate.

Acknowledgments

The authors would like to thank Prof. K. Sano, Department of Dentistry and Oral Surgery, Fukui Medical College for his excellent technical assistance. We also thank Dr. A, Kitamura, M,Uehara, N.Kamasaki and A. Fujisawa for their help in the passage of NR-S1 tumor cells and NB-1 tumor cell lines, and Dr. S. Ohba for his skillful technical assistance with the Western blotting method.

References

1. Hoye RC, Herrold K, Smith RR, *et al.* A clinicopathological study of epidermoid carcinoma of the head and neck. *Cancer* 1962; **15**: 741-9.
2. Cady B and Catlin D. Epidermoid carcinoma of the gum: a 20 year- survey. *Cancer* 1969; **23**: 551-9.
3. Harrold CC. Management of cancer of the floor of the mouth. *Am J Surg* 1971; **122**: 487-95.
4. Semba I, Matsuuchi H and Miura Y. Histomorphometric analysis of osteoclastic resorption in bone directly invaded by gingival squamous cell carcinoma. *J Oral Pathol Med* 1996; **25**: 429-35.
5. Belanger LF. Osteocytic Osteolysis. *Calc Tiss Res* 1969; **4**: 1-12.
6. Kawamata H, Nakashiro K, Uchida D, *et al.* Possible contribution of Active MMP2 to lymph-node metastasis and secreted cathepsin L to bone invasion of newly established human oral-squamous cancer cell lines. *Int J Cancer* 1997; **70**: 120-7.
7. Totsuka Y, Amemiya A and Tomita K. Histopathologic study of bone invasion by DMBA-induced carcinoma of the mouth in the hamster. *Oral Surg Oral Med Oral Pathol* 1986; **62**: 683-92.
8. Usui Y, Kawai K and Hirohata K. An electron microscopic study of the changes observed in osteocytes under ischemic conditions. *J Orthopaedic Res* 1989; **7**: 12-21.

9. Hamaya M, Mizoguchi Y, Sakakura Y, *et al*. Cell death of osteocytes occurs in rat alveolar bone during experimental tooth movement. *Calcif Tissue Int* 2002; **70**: 117-26.
10. Eilon G and Mundy GR. Direct resorption of bone by human breast cancer cells *in vitro*. *Nature* 1978; **276**: 726-8.
11. Tsao SW, Burman JF, Easty DM, *et al*. Some mechanisms of local bone destruction by squamous cell carcinomas of the head and neck. *Br J Cancer* 1981; **43**: 392-401.
12. Cramer SF, Fried L and Carter KJ. The cellular basis of metastatic bone disease in patients with lung cancer. *Cancer* 1981; **48**: 2649-60.
13. Tsao SW, Burman JF, Pittam MR, *et al*. Further observations on mechanisms of bone destruction by squamous carcinomas of the head and neck: the role of host stroma. *Br J Cancer* 1983; **48**: 697-704.
14. Aoki J, Yamamoto I, Hino M, *et al*. Osteoclast-mediated osteolysis in bone metastasis from renal cell carcinoma. *Cancer* 1988; **62**: 98-104.
15. Crowe DL and Shuler CF. Regulation of tumor cell invasion by extracellular matrix. *Histol Histopathol* 1999; **14**: 665-71.
16. Ohtani H and Ooshima A. Immunoelectron microscopic localization of human type III collagen in human gastrointestinal carcinomas. *Acta Pathol Jpn* 1990; **40**: 327-34.
17. Morino M, Tsuzuki T, Ishikawa Y, *et al*. Specific expression of HSP47 in human tumor cell lines *in vitro*. *In Vivo* 1997; **11**: 17-21.
18. Lin WL, McCulloch CAG and Cho MI. Differentiation of periodontal ligament fibroblasts into osteoblasts during socket healing after tooth extraction in the rat. *Anat Rec* 1994; **240**: 492-506.
19. Usui S, Urano M, Koike S, *et al*. Effect of PS-K, a protein polysaccharide, on pulmonary metastases of a C3H mouse squamous cell carcinoma. *J Natl Cancer Inst* 1976; **56**: 185-7.
20. Urano M, Nesumi N, Ando, K, *et al*. Repair of potentially lethal radiation damage in acute and chronically hypoxic tumor cells *in vivo*. *Radiology* 1976; **118**: 447-51.
21. Barka T and Anderson PJ. Histochemical methods for acid phosphatase using hexasonium pararosanilin as coupler. *J Histochem Cytochem* 1962; **10**: 741-53.
22. Gavrieli Y, Sherman Y and Ben-Sasson SA. Identification of programmed cell death *in situ* via specific labeling of nuclear DNA fragmentation. *J Cell Biol* 1992; **119**: 493-501.
23. Galasko CS, Rawlins R and Bennett A. Timing of indomethacin in the control of prostaglandins, osteoclasts and bone destruction produced by VX2 carcinoma in rabbits. *Br J Cancer* 1979; **40**: 360-4.
24. Georges E, Pehau-Arnaudet G, and Orth G. Molecular and biological characterization of cottontail rabbit papillomavirus variant DNA sequences integrated in the VX7 carcinoma. *Virology* 1992; **186**: 750-9
25. Ma G, Sano K, Ikeda H, *et al*. Promotional effects of CO_2 laser and scalpel incision on 4-NQO-induced premalignant lesions of mouse tongue. *Lasers Surg Med* 1999; **25**: 207-12.
26. Galasko CSB. Mechanism of bone destruction in the development of skeletal metastases. *Nature* 1976; **263**: 507-8.
27. Carter RL, Tsao SW, Burman JF, *et al*. Patterns and mechanism of bone invasion by squamous cell carcinoma of the head and neck. *Am J Surg* 1983; **146**: 451-5.
28. Quinn JM, McGee JOD and Athanasou NA. Human tumour-associated macrophages differentiate into osteoclastic bone-resorbing cells. *J Pathol* 1998; **184**: 31-6.
29. Boissier S, Ferreras M, Peyruchaud O, *et al*. Bisphosphonates inhibit breast and prostate carcinoma cell invasion, an early event in the formation of bone metastasis. *Cancer Res* 2000; **60**: 2949-54.
30. Okamoto M, Hiura K, Ohe G, *et al*. Mechanism for bone invasion of oral cancer cells mediated by interleukin-6 *in vitro* and *in vivo*. *Cancer* 2000; **89**: 1966-75.
31. Tumber A, Morgan HM, Meikle C, *et al*. Human breast-cancer cells stimulate the fusion, migration and resorptive activity of osteoclasts in bone explants. *Int J Cancer* 2001; **91**: 665-72.
32. Aznavoorian S, Moore BA, Alexande-Lister LD, *et al*. Membrane type I-metalloproteinase-mediated degradation of type I collagen by oral squamous cell carcinoma cells. *Cancer Res* 2001; **61**: 6264-75.
33. Knothe Tate ML, Nieederer P and Knothe U. *In vivo* tracer transport through the lacunocanalicular system of rat bone in an environment devoid of mechanical loading. *Bone* 1998; **22**: 107-17.
34. Hirsch T, Marchetti P, Susin SA, *et al*. The apoptosis-necrosis paradox. Apoptogenic proteases activated after mitochondrial permeability transition determine the mode of cell death. *Oncogene* 1997; **15**: 1573-81.
35. Barsky SH and Gopalakrishna R. Increased invasion and spontaneous metastasis of BL6 melanoma with inhibition of the desmoplastic response in C57 BL/6 mice. *Cancer Res* 1987; **47**: 1663-7.
36. Yamamoto M, Sumiyoshi H, Nakagami K, *et al*. Distribution of collagen types I and III and basal lamina in human gastric carcinoma: an immunohistochemical and electron microscopic study. *Virchows Arch A Pathol Anat Histopathol* 1984; **403**: 313-22.
37. Takechi H, Hirayoshi K, Nakai A, *et al*. Molecular cloning of a mouse 47-kDa heat- shock protein (HSP47), a collagen-binding stress protein, and its expression during the differentiation of F9 tetratocarcinoma cells. *Eur J Biochem* 1992; **206**: 323-9.
38. Hebert C, Norris K, Coletta RD, *et al*. Cell surface Colligin/Hsp47 with tetraspanin protein CD9 in epidermoid carcinoma cell lines. *J Cellular Biochem* 1999; **73**: 248-58.
39. Morino M, Yasuda T, Shirakami T, *et al*. HSP47 as a possible marker for malignancy of tumors *in vivo*. *In Vivo* 1994; **8**: 285-8.
40. Eisma RJ, Spiro JD and Kreutzer DL. Vascular endotherial growth factor expression in head and neck squamous cell carcinoma. *Am J Surg* 1997; **174**: 513-7.

(Accepted for publication December 24, 2002)